Int J Clin Exp Med 2015;8(2):1834-1843
www.ijcem.com /ISSN:1940-5901/IJCEM0003526

Original Article

Abnormal expression of NSF, α-SNAP and SNAP23 in pulmonary arterial hypertension in rats treated with monocrotaline

Hong-Liang Zhang, Zhi-Hong Liu, Qin Luo, Yong Wang, Zhi-Hui Zhao

State Key Laboratory of Cardiovascular Disease, Center for Pulmonary Vascular Diseases, Fuwai Hospital, National Center for Cardiovascular Diseases, Chinese Academy of Medical Sciences and Peking Union Medical College, Beijing 100037, People's R China

Received November 1, 2014; Accepted January 21, 2015; Epub February 15, 2015; Published February 28, 2015

Abstract: Background: Recent researches have shown that dysfunctional intracellular vesicular trafficking exists in pulmonary arterial hypertension (PAH). However, the expression of proteins involved in intracellular vesicular trafficking in pulmonary vasculature in PAH remains unclear. Objective: To elucidate possible roles of proteins involved in intracellular vesicular trafficking in the development of PAH in rats treated with monocrotaline, changes in the expression of N-ethyl-maleimide-sensitive factor (NSF), α-soluble NSF attachment protein (α-SNAP) and synaptosome-associated membrane protein (SNAP) 23 were examined together with expression of caveolin-1 (cav-1), endogenous nitric oxide synthase (eNOS), type 2 bone morphogenetic receptor (BMPR2) and cellular apoptosis. Methods: The mRNA expression was investigated by real time-PCR and protein expression by immunoblot method in rat lung. Caspase-3 was used as an indicator of cellular apoptosis and examined by immunoblot method. Results: During the development of PAH, mRNA and protein expression of NSF, α-SNAP and SNAP23 all significantly increased before pulmonary arterial pressure started to increase, then all significantly decreased when PAH established. The expression of eNOS and BMPR2 changed similarly, while the mRNA and protein of cav-1 both downregulated after monocrotaline treatment. Caspase-3 was also increased after exposure to monocrotaline. Conclusions: Since the expression of NSF, α-SNAP and SNAP23 changed greatly during the onset of PAH and accompanied with abnormal expression of eNOS, BMPR2 and cav-1 and with enhanced cellular apoptosis, NSF, α-SNAP and SNAP23 appear to be associated with the development of PAH in rats treated with monocrotaline.

Keywords: Pulmonary arterial hypertension, monocrotaline, intracellular vesicular trafficking

Introduction

Pulmonary arterial hypertension (PAH) is a syndrome resulting from restricted flow through the pulmonary arterial circulation resulting in increased pulmonary vascular resistance and ultimately in right heart failure [1]. Prior to 2003, primary pulmonary hypertension was used to describe idiopathic PAH and familial PAH. The pathology of PAH is characterized by abnormal expansions of endothelial cells, medial hypertrophy, and adventitial thickening of pulmonary arteries which lead to reduced arterial lumen, cycles of thrombosis and recanalization, and eventually to progressive right ventricular hypertrophy and cardiac failure [2, 3]. Before the era of target therapy (Endothelin antagonist, prostacyclin analogue, phosphodiesterase inhibitor), the medical management of PAH was directed at vasodilatation and anticoagulation, the median survival for PPH is only 2.8 years, and the 1-, 3-, 5-year survival rates were 68%, 48%, 34% respectively [4]. Even with modern target therapy, for patients with idiopathic/familial PAH, the median survival is 7 years, and 1-, 3-, 5-, and 7-year survival rates were 91%, 74%, 65%, and 59%, respectively [5].

The past studies showed that the hallmark plexiform lesions in PAH consisted of enlarged endothelial cells, fibroblasts, and smooth muscle cell elements, which contained increased endoplasmic reticulum, Golgi stacks, vacuolation and Weibel-Palade bodies [6-8]. These

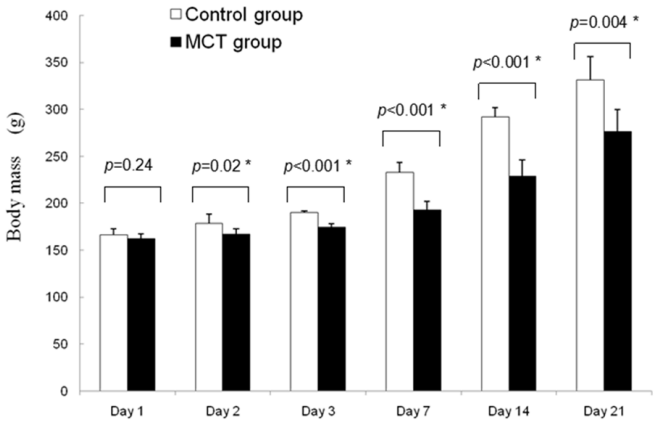

Figure 1. The body mass of each rat was weighed on the 1, 2, 3, 7, 14, 21 day after MCT or normal saline treatment. The body mass was significantly lower in MCT group than in controls from the second day after treatment. *P < 0.05 vs. control. #P < 0.01 vs. control.

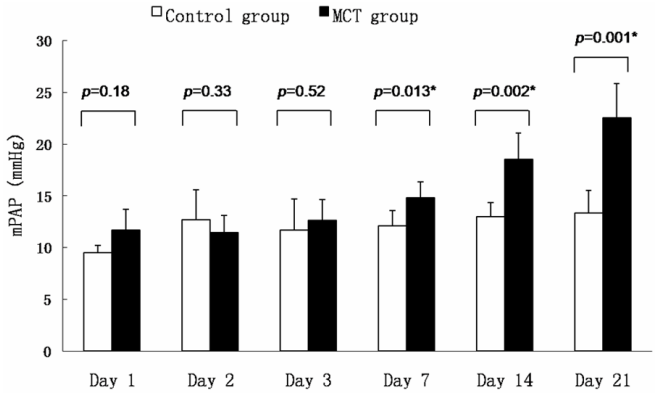

Figure 2. The mean pulmonary arterial pressure of each rat was measured on the 1, 2, 3, 7, 14, 21 day after MCT or normal saline treatment. The mean pulmonary arterial pressure progressively increased from Day 7 after treatment and was highest on Day 21. *P < 0.05 vs. control. #P < 0.01 vs. control.

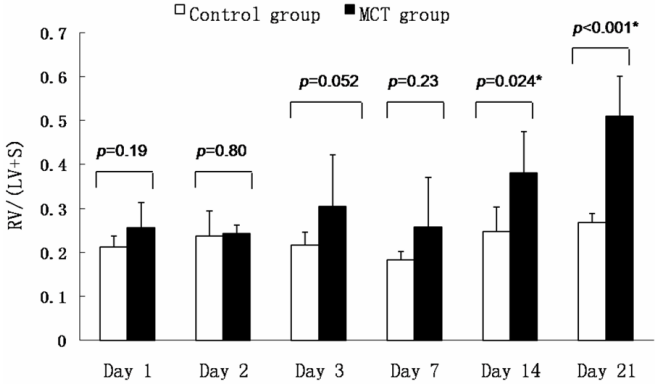

Figure 3. The weight ratio of right ventricle to left ventricle plus septum [RV/(LV+S)] of each rat was measured on the 1, 2, 3, 7, 14, 21 day after MCT or normal saline treatment. RV/(LV+S) gradually elevated from Day 14 after treatment and was also highest on Day 21. *P < 0.05 vs. control. #P < 0.01 vs. control.

findings also applied to experimental PAH models [9-12]. Recent researches observed trapping of various vesicle trafficking tethers, soluble N-ethyl-maleimide-sensitive factor attachment proteins (SNAPs) and membrane proteins which serve as SNAP receptors (SNAREs), loss or reduction of cell surface protein from plasma membrane (e.g. caveolin-1 (cav-1), endogenous nitric oxide synthase (eNOS), type 2 bone morphogenetic receptor (BMPR2)) with the aberrant sequestration in the endoplasmic reticulum, Golgi apparatus and in cytoplasmic vesicles in PAH lesions. This resulted in reduced cell surface/caveolar production of NO, hypo-S-nitrosylation of the trafficking mediator proteins, hyperactivation of STAT3 and defect in BMP/Smad signaling, imbalance of cellular proliferation and apoptosis [13-15]. All these findings points to dysfunctional intracellular vesicular trafficking within the cellular elements in the arterial lesions in PAH. However, the expression of proteins associated with intracellular vesicular trafficking is unclear in PAH. In present research, changes in the temporal expression of proteins associated with intracellular vesicular trafficking (N-ethyl-maleimide-sensitive factor (NSF), α-SNAP and SNAP23 (here SNAP stands for synaptosome-associated membrane protein, belongs to SNAREs) were investigated in rats treated with monocrotaline (MCT) for 1-21 days together with changes in the expression of membrane proteins (cav-1, eNOS and BMPR2) and cellular apoptosis.

Methods

Animal

Seventy-eighty pathogen-free, 6-7 week old, male Sprague-Dawley rats (body weight, 160-180 g) (Vital River Lab Animal Technology Co., Ltd., Beijing, China) were studied. All protocols and procedures were reviewed and approved by the Institutional Animal Use Committee of Fuwai Hospital & Cardiovascular Institute, Chinese Academy of Medical Sciences & Peking Union Medical College in accordance with the Regulations for the Administration of Affairs Concerning Experi-

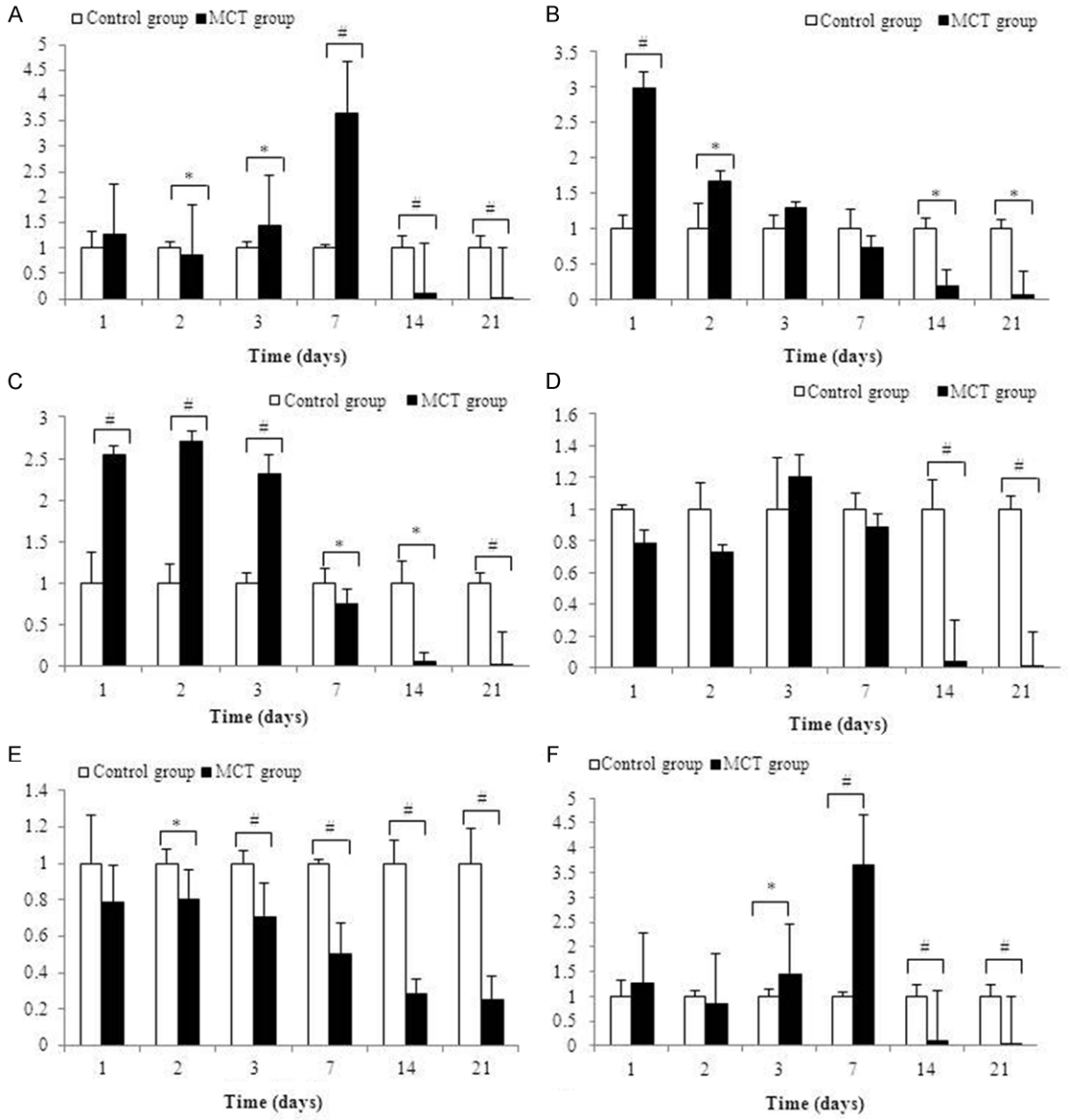

Figure 4. The mRNA expression of NSF (A), α-SNAP (B), SNAP23 (C), BMPR2 (D), caveolin-1 (E) and eNOS (F) were analyzed by semiquantitative Real Time PCR. The rats were harvested on the 1, 2, 3, 7, 14, 21 day after MCT or normal saline treatment. The data represent results of 3 separate experiments. *P < 0.05 vs. control. #P < 0.01 vs. control.

mental Animals approved by the State Council and promulgated by the State Science and Technology Commission of China. The investigation conformed to the Guidelines for the Care and Use of Laboratory Animals, as published by the National Academy Press (NIH Publication No. 85-23, revised 1985).

Animal treatment

Rats were equally randomized to 6 groups, in each group 9 rats were given MCT (Sigma, St. Louis, MO, USA) and 4 rate were given same amount of normal saline as controls intraperitoneally (60 mg/kg). MCT was dissolved in distilled water, adjusted to pH 7.40 with 0.5 N HCl and injected intraperitoneally. Then rats in each group were randomly sacrificed on Day 1, Day 2, Day3, Day 7, Day 14 and Day 21 after injection, respectively.

Hemodynamic studies and tissue preparation

Rats were anesthesized by intraperitoneal injections of chloral hydrate (2.5 mg/kg), placed in the supine position, intubated and ven-

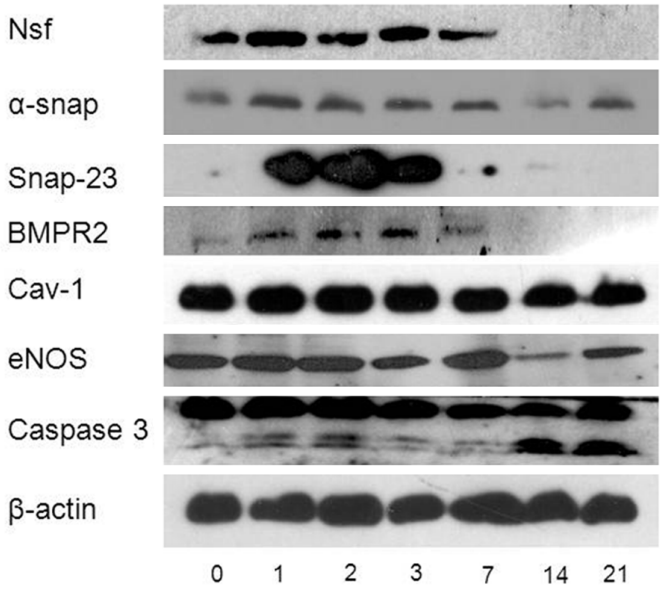

Figure 5. The protein expression of NSF, α-SNAP, SNAP23, BMPR2, caveolin-1 and eNOS were analyzed by immunoblot analysis. The rats were harvested on the 1, 2, 3, 7, 14, 21 day after MCT or normal saline treatment. The data represent results of 3 separate experiments. *P < 0.05 vs. control. #P < 0.01 vs. control.

tilated with room air at 60 breaths/min with a pressure-cycled rodent ventilator (Zhe Jiang Medical University Laboratory Apparatus Factory, Hangzhou, China). After sternal incision, a percutaneous needle (27 gauge) connected with transducer and flushed with heparinized saline was directly punctured into pulmonary artery to measure pulmonary pressure. The correct positioning of the needle in pulmonary artery was confirmed by pressure wave before pulmonary arterial pressure was recorded. After exsanguination, the lungs were perfused with heparinized saline through the needle; then the right lung, right ventricle, and left ventricle plus septum were collected. The lungs were axially sectioned, rapidly frozen in liquid nitrogen and stored at -80°C until analysis and determination of total cellular RNA and tissue protein. Right ventricle and left ventricle plus septum were weighted. Development of pulmonary hypertension was determined by the pulmonary arterial pressure and the weight ratio of the right ventricle over the left ventricle plus septum [RV/(LV+S)].

Real time PCR analysis

The mRNA expression of vesicular trafficking proteins (NSF, α-snap, SNAP 23) and plasma membrane proteins (eNOS, Cav-1 and BMPR2.) was evaluated with semiquantitative Real Time-PCR. Total RNA was isolated from rat lungs with the SV Total RNA Isolation System (Z3100, Promega, USA), and then the RNA sample was reverse transcribed with the Reverse Transcription System (A3500, Promega, USA) in 20 μl according to the manufacturer's instructions. PCR was conducted at linearity phase of the exponential reaction for each gene. The cDNA was amplified using SYBR® Green Realtime PCR Master Mix (QPK-201, TOYOBO, Japan) in 20 μl according to the manufacturer's instructions with the following program: 1 cycle of 95°C for 60 s; 40 cycles of 95°C for 15 s and 56°C for 60 s. The amplification of the target genes was conducted on a 7300 real-time PCR system (Applied Biosystems) and monitored every cycle by SYBR-green fluorescence.

Western blotting

For each assay, frozen lung tissues were homogenized by cooled RIPA protein extract solution (30 mM Tris, 150 mM NaCl, 1 mM benzylsulfonyl fluoride, 1 mM Na3V04, 1% Nonidet P-40, 10% glycerol, and pH 7.5) with PMSF (100 mM), then centrifugation at 12,000 g for 20 min at 4°C, the concentration of protein was quantified by BCA protein assays. Equal amounts of protein (50 μg/lane) were separated by electrophoresis through 12% sodium dodecyl sulfate polyacrylamide gel (60 V for 2 h) in a Tris/HCl buffer system, and transferred to nitrocellulose membranes (Millipore, USA) using an semi-dry elecroblotting apparatus (Bio-Rad, USA) for 25 min at 25 V, then blocked the membrane with 5% skim milk for 1 h at room temperature. Then nitrocellulose membranes were incubated with monoclonal mouse antibody against NSF (1:500, Abcom Inc.), α-SNAP (1:500, Santa Cruz BioTechnology, Inc.), polyclonal goat antibody against SNAP23 (1:100, Santa Cruz BioTechnology, Inc.), BMPR2 (1:100, BD Biosciences), cav-1 (1:1000, LifeSpan BioSciences, Inc.), eNOS (1:100, BD Biosciences) or polyclonal mouse antibody against caspase3 (1:500, all from Santa Cruz BioTechnology, Inc.) at 4°C overnight. After incubation, membranes were washed in PBS, and probed with secondary antibodies conju-

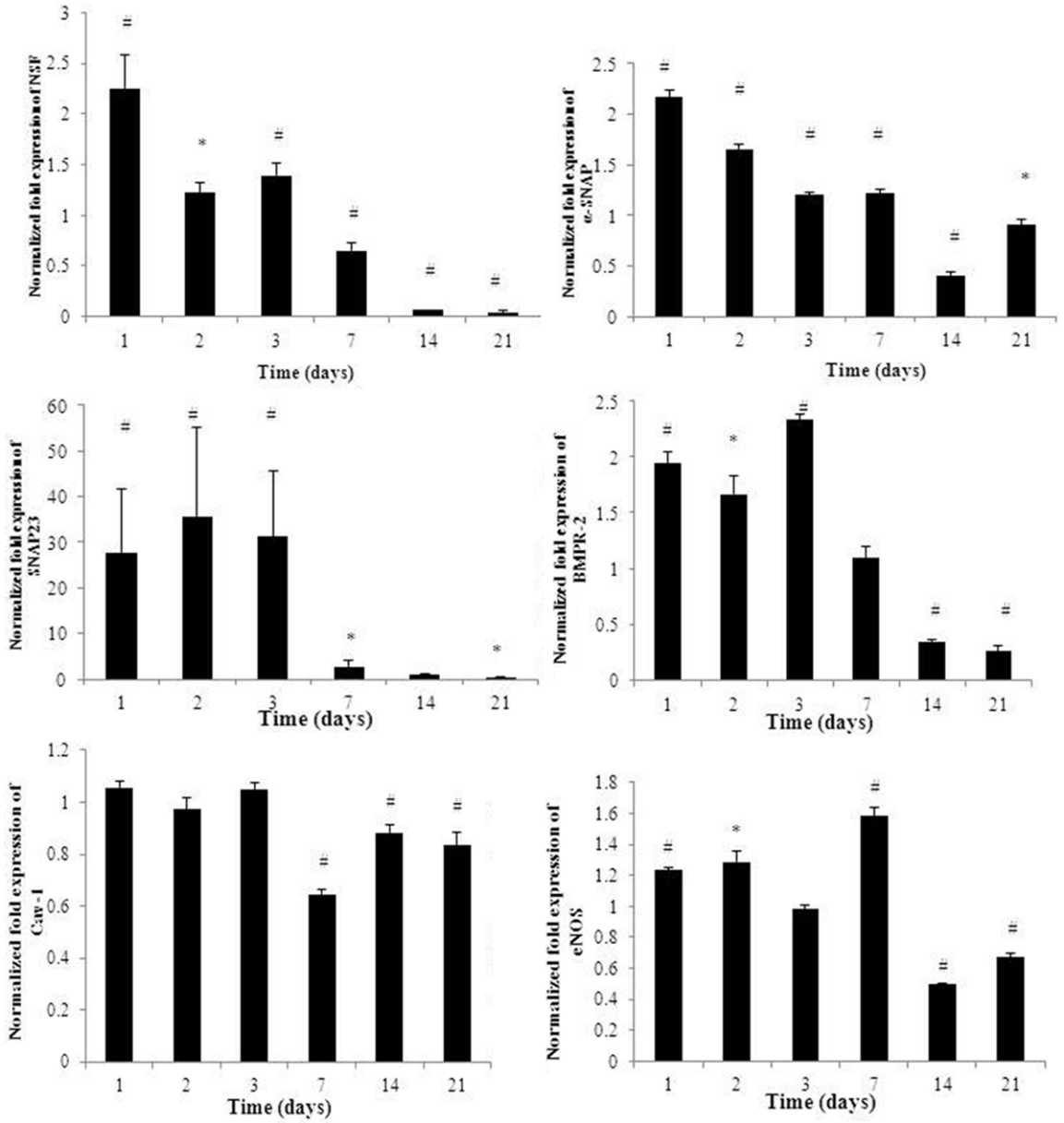

Figure 6. Cellular apoptosis was analyzed by immunoblot analysis. The rats were harvested on the 1, 2, 3, 7, 14, 21 day after MCT or normal saline treatment. Compared to controls, The 20- and 17-kDa bands for the active form and a 32-kDa band for the inactive form of caspase-3 was increased after exposure to MCT and was highest on days 14 and 21.

gated with horseradish peroxides (1:5000, Protein Tech). Specific bands of target proteins were visualized by chemilominescence. Target signals were normalized to the β-actin (1:2000, Protein Tech) signal and analyzed semiquantitatively with Quantity One system.

Statistical analysis

Numerical data are presented as means ± standard deviation. Comparisons between groups were made with Student's t-test. Differences among groups were tested by one-way ANOVA. Two sided *P* values were used. A value of $P < 0.05$ was considered significant.

Results

Pulmonary arterial hypertension was successfully established

At baseline the body mass did not differ in all the 6 groups (Day 1 to Day 21) ($F = 2.33$, $P = 0.051$), while the body mass was significantly lower in MCT group than in controls from Day 2 after injection, which means that MCT lead to

growth retardation of the rats (**Figure 1**). Compared to controls, the mean pulmonary arterial pressure progressively increased from Day 7 after injection and was highest on Day 21 (Day 7: 14.83 ± 1.54 mm Hg vs. 12.13 ± 1.44 mm Hg, P = 0.013; Day 14: 18.56 ± 2.53 mm Hg vs. 13 ± 1.35 mm Hg, P = 0.002; Day 21: 22.57 ± 3.25 mm Hg vs. 13.38 ± 2.17 mm Hg, P = 0.001) (**Figure 2**). While measurement of ventricular weights revealed that the ratio of RV/(LV+S) gradually elevated from Day 14 after injection and was also highest on Day 21 (Day 14: 0.38 ± 0.09 vs. 0.25 ± 0.06, P = 0.024; Day 21: 0.5 ± 0.09 vs. 0.27 ± 0.02, P < 0.001) (**Figure 3**), which indicated that the development of PAH results in a compensatory hypertrophy of the right ventricle.

Time courses and effects of MCT on mRNA expression of NSF, α-SNAP, SNAP23, BMPR2, cav-1 and eNOS

Semiquantitative Real Time-PCR analysis was utilized to detect changes in mRNA expression of NSF, α-SNAP, SNAP23, BMPR2, Cav-1 and eNOS in rat lung tissues after exposure to MCT (**Figure 4**). Housekeeping gene glyc-eraldehyde-3 phosphate dehydrogenase (GAPDH) were used as an internal control. Compared with control rats, NSF increased from the second day after exposure to MCT, was highest on the 7th day (9.2 fold, P < 0.001), then significantly decreased from the 14th day to a level hardly detected. α-SNAP level increased on Day 1 (3 fold, P = 0.004) and Day 2 (1.7 fold, P = 0.019), returned to control levels from Day 3 , then greatly decreased from Day 14. The mRNA expression of SNAP23 was approximately 2-3 fold greater on the first 3 days after MCT treatment, then started to decrease from Day 7, and was hardly detected on Day 14 and 21. The mRNA expression of BMPR2 did not change significantly during Day 1-7 (0.7-1.2, P = 0.05-0.23), then significantly decreased from Day 14-21. Except for the first day, cav-1 gradually decreased during exposure to MCT to 25% of the control level on Day 21. eNOS was elevated on Day 3 and 7 (1.4-3.7 fold), started to decline from Day 14 and hardly detected onf Day 21.

Time courses and effects of MCT on protein expression of NSF, α-SNAP, SNAP23, BMPR2, cav-1 and eNOS

We identified 76 kDA bands for NSF, 38 kDA bands for α-SNAP, 23 kDA bands for SNAP23, 130 kDA bands for BMPR2, 22 kDA bands for cav-1 and 140-kDA bands for eNOS proteins in lung tissue from rats by Western immunoblotting analysis (**Figure 5**). Compared with controls, NSF increased during exposure to MCT on Day 1-3 (1.2-2.3 fold, P < 0.05), then significantly decreased from Day 7 and hardly detected after 14-21 days. α-SNAP levels were 1.2-2.2 fold increased from 1 to 7 days after MCT treatment (P < 0.01), then significantly decreased from the 14th day after MCT treatment. SNAP23 protein levels significantly increased on the first 7 days (approximately 3-36 fold, P < 0.05), decreased to control level on the 14th day and then significantly reduced on Day 21. BMPR2 level was upregulated by 1.7-2.3 fold on Day 1-3 (P ≤ 0.01), returned to control level on Day 7 (P = 0.41), then significantly reduced (P < 0.01). The expression of cav-1 was downregulated from the second day after MCT treatment (0.6-0.9 fold, P < 0.01), except on the 3 day (P = 0.06). The protein level of eNOS elevated 1.2-1.6 fold during Day 1 to 7 (P < 0.05) except on the third day (0.98 fold, p = 0.38), then reduced by 34-50% after 14-21 days (P < 0.01).

Time course and effects of MCT on activation of caspase-3

As we know, abnormal apoptosis plays an important role in the pathogenesis of PAH. In order to analyze the relationship between the expression of vesicular trafficking protein and cellular apoptosis, we next investigated the expression of caspase-3, which is known as an important effector enzyme for apoptosis, by Western blot analysis. The 20- and 17-kDa bands for the active form and a 32-kDa band for the inactive form of caspase-3 were constitutively expressed in rat lungs (**Figure 6**). Compared to controls, the active form of caspase-3 was increased after exposure to MCT and was highest on days 14 and 21.

Discussion

The transportation of proteins to the target subcellular compartments and organelles is mediated by intracellular membrane-vesicular trafficking and subsequent membrane fusion, which includes tether proteins, NSF, SNAPs and SNAREs [16-18]. The process is complicated. Briefly, tether proteins bring cargo vesicle and target membranes together, then respective

membrane is fused after formation of a complex by the SNARE proteins on the cargo vesicle and target membranes, subsequently SNAP protein (usually α-SNAP) recruits NSF to disassemble the complex for the next transportation [19-21]. Dysfunctional vesicular trafficking is the underlying cause of several diseases, such as Parkinson's disease, Alzheimer's disease, lysosomal storage diseases [16, 22]. Recent studies reported dysfunctional vesicular trafficking as a prelude to the development of PAH. We conducted this study to demonstrate the temporal expression of NSF, α-SNAP and SNAP23, together with the expression of eNOS, cav-1 and BMPR2 in lungs from normal rats and animals treated with MCT. Our observations showed that NSF, α-SNAP and SNAP23 all upregulated preceding the appearance of PAH and downregulated when the pulmonary arterial pressure increased both at mRNA and protein level, and the similar changes appeared in the expression of BMPR2 and eNOS; while cav-1 was merely downregulated both in mRNA and protein expression. Caspase-3 was also increased after exposure to monocrotaline and greatly increased when PAH established.

NSF is an ATPase required for the disassembly of all SNARE complexes and can be covalently modified by NO-mediated S-nitrosylation to lose the ability to disassemble SNARE complexes [23]. α-SNAP is essential for the recruitment of NSF to SNARE complex [28, 29, 32]. SNAP23 forms clusters with syntaxin-4 in the plasma membrane served as the fusion sites for caveolae during exocytosis [24]. In experimental PAH, it was found that diverse tethers, SNAREs and SNAPs were trapped in Golgi together with eNOS, cav-1 and BMPR2, while NSF was found to be largely sequestered in an intracellular location separate from the Golgi, which suggested dysfunction in the disassembly step in vesicular trafficking [14, 15]. In our study, NSF, α-SNAP and SNAP23 were uniformly upregulated from the first day after administration of MCT, at a time largely preceding development of PAH, then started to decrease accompanied with increased pulmonary arterial pressure from the 7^{th} or 14^{th} day. These data suggested that such changes might lie in the pathogenesis of PAH and were not a consequence of increased pulmonary arterial pressure. The effect of upregulation of NSF, α-SNAP and SNAP23 is not clear. It was found that exogenous secretion was markedly increased from the second day and sustained for the duration of the 5-day assay in monocrotaline pyrolle and nitric oxide scavenger treated pulmonary arterial endothelial cells [13, 15]. Maybe there are some connections between these phenomenon. Studies have shown that the inward transcription-targeted signaling involving the Smad family and STAT3 transcription factors is associated with endocytic/caveolar vesicular trafficking, which must involve NSF, SNAREs, SNAPs, et al [25-28]. The downregulatin of NSF, α-SNAP and SNAP23 may lead to dysfunctional Smad and STAT3 signaling pathway which were known to participate the development of PAH. Actually we did find that cellular apoptosis was significantly increased when NSF, α-SNAP and SNAP23 were downregulated and pulmonary arterial pressure increased, their relationship worth further investigation. We made a hypothesis that there might be a feedback mechanism to the damaged vesicular trafficking caused by MCT. At first NSF, α-SNAP and SNAP23 were upregulated to maintain vesicular trafficking, but when decompensation their expression were downregulated, which can further aggravate the damaged vesicular trafficking and lead to elevated pulmonary arterial pressure in a self-reinforcing manner.

BMP is a member of the transforming growth factor-β family, binds to BMPR2, and activate Smad-family transcription factors to inhibit cellular proliferation. BMPR2 mutation accounts for approximately one-half of the familial cases and one-quarter of the sporadic PAH cases. Several mutant BMPR II species failed to traffic correctly to the plasma membrane with abnormal sequestration in the ER, Golgi or even those that traffic to the plasma membrane and yet exhibit defective signaling [29, 30]. It is reported that there are reduced levels of BMPR II and reduced BMP/Smad signaling even though there are no mutations in BMPR II in primary pulmonary hypertension [31]. As we know, Smad signaling is dependent on membrane-associated endocytic pathways. Defects in intracellular vesicular trafficking might explain defects in BMP/Smad signaling in IPAH despite no mutations in BMPR II. In our study BMPR2 was significantly increased during the first 3 days after MCT treatment only at the protein levels, meaning that upregulation of BMPR2 is at posttranslational level, not the mRNA, then

BMPR2 was downregulated from the 14th day after MCT treatment both at the mRNA and protein levels.

Caveolae are 50-100 nm invaginations of the plasma membrane that are enriched in cholesterol and sphingolipids. Caveolins are the structural proteins essential for the formation of caveolae in lipid raft domains. Caveolin-1 is highly expressed in endothelial cells, adipocytes, and smooth muscle cells. It was found that cav-1 was reduced in the cells in plexiform lesions in patients with PAH and rats treated with MCT, and cav-1-/- mice spontaneously developed pulmonary hypertension and dilated cardiomyopathy [32, 33]. Loss of cav-1 from cell surface inversely related with hyperactivation of promitogenic and antiapoptotic PY-STAT3 and ERK1/2 signaling and DNA synthesis and with development of PAH BMPR II is located in lipid rafts, including caveolae [34], and cav-1 can regulate the caveolar localization and transcriptional activation function of BMPR II [35]. Reduction in cav-1 or a dominant-negative mutant of cav-1 can reduce BMPR II plasma membrane localization, decreased BMP-dependent Smad phosphorylation and gene regulation [49]. We also found that cav-1 was downregulated in MCT treated rats, which may promote the formation of PAH through activation of PY-STAT3 and ERK1/2 signaling pathway and decreased BMP-Smad signaling pathway.

NO level is reduced in the pulmonary arterial walls in human and experimental PAH, however the levels of eNOS have been variably reported as unchanged, decreased, or even increased [36, 37]. In this study the expression of eNOS was upregulated at first and downregulated after pulmonary arterial pressure started to increase. The extracellular NO derives from cell-surface caveolar eNOS, while eNOS is found lost from cell surface caveolae and trapped in intracellular compartment, such as Golgi and endoplasmic reticulum [38]. NO can still be generated by eNOS but cannot reach the extracellular space leading to the reduced NO in the pulmonary arterial vasculature. The intracellular NO causes S-nitrosylation of NSF and further inhibits vesicular trafficking in a self-reinforcing inhibitory loop [36]. According to these findings, we speculate that increased eNOS may inhibit NSF leading to exacerbation of dysfunctional vesicular trafficking, and decreased eNOS level leads to shortage of NO which promotes the elevation of pulmonary arterial pressure.

In summary, we found that the expressions of NSF, α-SNAP and SNAP23 were upregulated preceding the formation of PAH and downregulated after PAH established both at mRNA and protein levels in MCT treatment rats, and accompanied with abnormal expression of BMPR2, cav-1 and eNOS and with enhanced cellular apoptosis. NSF, α-SNAP and SNAP23 appear to be associated with the development of PAH and their roles worth further study.

Acknowledgements

This study was supported by National Natural Science Foundation of China (Grant No. 308-71056).

Disclosure of conflict of interest

None.

Address correspondence to: Dr. Zhihong Liu, State Key Laboratory of Cardiovascular Disease, Center for Pulmonary Vascular Diseases, Fuwai Hospital, National Center for Cardiovascular Diseases, Chinese Academy of Medical Sciences and Peking Union Medical College, Beilishi Road 167, Fuwai Hospital, Xicheng District, Beijing 100037, People's R China. Tel: +86 010 88396589; Fax: +86 010 88396589; E-mail: 330954476@qq.com

References

[1] McLaughlin VV, Archer SL, Badesch DB, Barst RJ, Farber HW, Lindner JR, Mathier MA, McGoon MD, Park MH, Rosenson RS, Rubin LJ, Tapson VF and Varga J. ACCF/AHA 2009 expert consensus document on pulmonary hypertension a report of the American College of Cardiology Foundation Task Force on Expert Consensus Documents and the American Heart Association developed in collaboration with the American College of Chest Physicians; American Thoracic Society, Inc.; and the Pulmonary Hypertension Association. J Am Coll Cardiol 2009; 53: 1573-1619.

[2] Humbert M, Morrell NW, Archer SL, Stenmark KR, MacLean MR, Lang IM, Christman BW, Weir EK, Eickelberg O, Voelkel NF and Rabinovitch M. Cellular and molecular pathobiology of pulmonary arterial hypertension. J Am Coll Cardiol 2004; 43: 13S-24S.

[3] Cool CD, Groshong SD, Oakey J and Voelkel NF. Pulmonary hypertension: cellular and molecular mechanisms. Chest 2005; 128: 565S-571S.

[4] D'Alonzo GE, Barst RJ, Ayres SM, Bergofsky EH, Brundage BH, Detre KM, Fishman AP, Goldring RM, Groves BM, Kernis JT, et al. Survival in patients with primary pulmonary hypertension. Results from a national prospective registry. Ann Intern Med 1991; 115: 343-349.

[5] Benza RL, Miller DP, Barst RJ, Badesch DB, Frost AE and McGoon MD. An evaluation of long-term survival from time of diagnosis in pulmonary arterial hypertension from the REVEAL Registry. Chest 2012; 142: 448-456.

[6] Heath D, Smith P, Gosney J, Mulcahy D, Fox K, Yacoub M and Harris P. The pathology of the early and late stages of primary pulmonary hypertension. Br Heart J 1987; 58: 204-213.

[7] Smith P and Heath D. Electron microscopy of the plexiform lesion. Thorax 1979; 34: 177-186.

[8] Smith P, Heath D, Yacoub M, Madden B, Caslin A and Gosney J. The ultrastructure of plexogenic pulmonary arteriopathy. J Pathol 1990; 160: 111-121.

[9] Merkow L and Kleinerman J. An electron microscopic study of pulmonary vasculitis induced by monocrotaline. Lab Invest 1966; 15: 547-564.

[10] Rosenberg HC and Rabinovitch M. Endothelial injury and vascular reactivity in monocrotaline pulmonary hypertension. Am J Physiol 1988; 255: H1484-1491.

[11] Meyrick B and Reid L. Hypoxia-induced structural changes in the media and adventitia of the rat hilar pulmonary artery and their regression. Am J Pathol 1980; 100: 151-178.

[12] Jaenke RS and Alexander AF. Fine structural alterations of bovine peripheral pulmonary arteries in hypoxia-induced hypertension. Am J Pathol 1973; 73: 377-398.

[13] Lee J, Reich R, Xu F and Sehgal PB. Golgi, trafficking, and mitosis dysfunctions in pulmonary arterial endothelial cells exposed to monocrotaline pyrrole and NO scavenging. Am J Physiol Lung Cell Mol Physiol 2009; 297: L715-728.

[14] Mukhopadhyay S, Xu F and Sehgal PB. Aberrant cytoplasmic sequestration of eNOS in endothelial cells after monocrotaline, hypoxia, and senescence: live-cell caveolar and cytoplasmic NO imaging. Am J Physiol Heart Circ Physiol 2007; 292: H1373-1389.

[15] Oh IJ, Kim HE, Song SY, Na KJ, Kim KS, Kim YC and Lee SW. Diagnostic value of serum glutathione peroxidase 3 levels in patients with lung cancer. Thoracic Cancer 2014; 5: 425-430.

[16] Cooper AA, Gitler AD, Cashikar A, Haynes CM, Hill KJ, Bhullar B, Liu K, Xu K, Strathearn KE, Liu F, Cao S, Caldwell KA, Caldwell GA, Marsischky G, Kolodner RD, Labaer J, Rochet JC, Bonini NM and Lindquist S. Alpha-synuclein blocks ER-Golgi traffic and Rab1 rescues neuron loss in Parkinson's models. Science 2006; 313: 324-328.

[17] Fries E and Rothman JE. Transport of vesicular stomatitis virus glycoprotein in a cell-free extract. Proc Natl Acad Sci U S A 1980; 77: 3870-3874.

[18] Gissen P, Johnson CA, Morgan NV, Stapelbroek JM, Forshew T, Cooper WN, McKiernan PJ, Klomp LW, Morris AA, Wraith JE, McClean P, Lynch SA, Thompson RJ, Lo B, Quarrell OW, Di Rocco M, Trembath RC, Mandel H, Wali S, Karet FE, Knisely AS, Houwen RH, Kelly DA and Maher ER. Mutations in VPS33B, encoding a regulator of SNARE-dependent membrane fusion, cause arthrogryposis-renal dysfunction-cholestasis (ARC) syndrome. Nat Genet 2004; 36: 400-404.

[19] Stow JL, Manderson AP and Murray RZ. SNAREing immunity: the role of SNAREs in the immune system. Nat Rev Immunol 2006; 6: 919-929.

[20] Jahn R and Scheller RH. SNAREs--engines for membrane fusion. Nat Rev Mol Cell Biol 2006; 7: 631-643.

[21] Bonifacino JS and Glick BS. The mechanisms of vesicle budding and fusion. Cell 2004; 116: 153-166.

[22] Suzuki T, Araki Y, Yamamoto T and Nakaya T. Trafficking of Alzheimer's disease-related membrane proteins and its participation in disease pathogenesis. J Biochem 2006; 139: 949-955.

[23] Matsushita K, Morrell CN, Cambien B, Yang SX, Yamakuchi M, Bao C, Hara MR, Quick RA, Cao W, O'Rourke B, Lowenstein JM, Pevsner J, Wagner DD and Lowenstein CJ. Nitric oxide regulates exocytosis by S-nitrosylation of N-ethylmaleimide-sensitive factor. Cell 2003; 115: 139-150.

[24] Predescu SA, Predescu DN, Shimizu K, Klein IK and Malik AB. Cholesterol-dependent syntaxin-4 and SNAP-23 clustering regulates caveolar fusion with the endothelial plasma membrane. J Biol Chem 2005; 280: 37130-37138.

[25] Di Guglielmo GM, Le Roy C, Goodfellow AF and Wrana JL. Distinct endocytic pathways regulate TGF-beta receptor signalling and turnover. Nat Cell Biol 2003; 5: 410-421.

[26] Sehgal PB, Guo GG, Shah M, Kumar V and Patel K. Cytokine signaling: STATS in plasma membrane rafts. J Biol Chem 2002; 277: 12067-12074.

[27] Shah M, Patel K, Mukhopadhyay S, Xu F, Guo G and Sehgal PB. Membrane-associated STAT3 and PY-STAT3 in the cytoplasm. J Biol Chem 2006; 281: 7302-7308.

[28] Xu F, Mukhopadhyay S and Sehgal PB. Live cell imaging of interleukin-6-induced targeting of

"transcription factor" STAT3 to sequestering endosomes in the cytoplasm. Am J Physiol Cell Physiol 2007; 293: C1374-1382.
[29] Morrell NW. Role of bone morphogenetic protein receptors in the development of pulmonary arterial hypertension. Adv Exp Med Biol 2010; 661: 251-264.
[30] Nishihara A, Watabe T, Imamura T and Miyazono K. Functional heterogeneity of bone morphogenetic protein receptor-II mutants found in patients with primary pulmonary hypertension. Mol Biol Cell 2002; 13: 3055-3063.
[31] Atkinson C, Stewart S, Upton PD, Machado R, Thomson JR, Trembath RC and Morrell NW. Primary pulmonary hypertension is associated with reduced pulmonary vascular expression of type II bone morphogenetic protein receptor. Circulation 2002; 105: 1672-1678.
[32] Zhao YY, Liu Y, Stan RV, Fan L, Gu Y, Dalton N, Chu PH, Peterson K, Ross J Jr and Chien KR. Defects in caveolin-1 cause dilated cardiomyopathy and pulmonary hypertension in knockout mice. Proc Natl Acad Sci U S A 2002; 99: 11375-11380.
[33] Zhao YY, Zhao YD, Mirza MK, Huang JH, Potula HH, Vogel SM, Brovkovych V, Yuan JX, Wharton J and Malik AB. Persistent eNOS activation secondary to caveolin-1 deficiency induces pulmonary hypertension in mice and humans through PKG nitration. J Clin Invest 2009; 119: 2009-2018.
[34] Ramos M, Lame MW, Segall HJ and Wilson DW. The BMP type II receptor is located in lipid rafts, including caveolae, of pulmonary endothelium in vivo and in vitro. Vascul Pharmacol 2006; 44: 50-59.
[35] Wertz JW and Bauer PM. Caveolin-1 regulates BMPRII localization and signaling in vascular smooth muscle cells. Biochem Biophys Res Commun 2008; 375: 557-561.
[36] Giaid A and Saleh D. Reduced expression of endothelial nitric oxide synthase in the lungs of patients with pulmonary hypertension. N Engl J Med 1995; 333: 214-221.
[37] Tyler RC, Muramatsu M, Abman SH, Stelzner TJ, Rodman DM, Bloch KD and McMurtry IF. Variable expression of endothelial NO synthase in three forms of rat pulmonary hypertension. Am J Physiol 1999; 276: L297-303.
[38] Murata T, Sato K, Hori M, Ozaki H and Karaki H. Decreased endothelial nitric-oxide synthase (eNOS) activity resulting from abnormal interaction between eNOS and its regulatory proteins in hypoxia-induced pulmonary hypertension. J Biol Chem 2002; 277: 44085-44092.